Photoacoustic generation of focused quasi-unipolar pressure pulses

Konstantin Maslov[a], **Hao F. Zhang**[b], and **Lihong V. Wang**[a,£]

[a]Optical Imaging Laboratory, Department of Biomedical Engineering, Washington University in St. Louis, St. Louis, Missouri 63130

Abstract

The photoacoustic effect was employed to generate short-duration quasi-unipolar acoustic pressure pulses in both planar and spherically focused geometries. In the focal region, the temporal profile of a pressure pulse can be approximated by the first derivative of the temporal profile near the front transducer surface, with a time averaged value equal to zero. This approximation agreed with experimental results acquired from photoacoustic transducers with both rigid and free boundaries. For a free boundary, the acoustic pressure in the focal region is equal to the sum of a positive pressure that follows the spatial profile of the optical energy deposition in the medium and a negative pressure that follows the temporal profile of the laser pulse.

Keywords

Photoacoustics; Optoacoustics; Ultrasound generation

Introduction

The photoacoustic (PA) effect is widely used for imaging of optical contrast in biological tissues. In this case focused ultrasonic transducer is used to localize optical absorption by detecting pressure generated by thermal expansion of the tissue caused by absorbed pulsed laser energy. Alternatively, PA effect can be used to generate localized pressure pulses of a predictable shape, for example, quasi-unipolar pressure pulses, for therapeutic or diagnostic purposes.

Short unipolar pressure pulses can be used to improve the spatial resolution of ultrasonic imaging [1–3] and to produce controllable damages in biological tissue based on nonlinear acoustic effects, such as cavitation [4,5]. However, generating unipolar pressure pulses using traditional piezoelectric methods presents several difficulties because of the large frequency bandwidths that unipolar pulses contain. If a transducer is made from thin piezoelectric material operating around its resonance frequency, the transducer acts as a band-pass filter with a narrow bandwidth, which makes it impossible to generate a unipolar pulse [1].

There are several methods to generate unipolar pressure pulses by altering the geometry of the piezoelectric material or controlling the driving voltage [6–8]. One method is to use thick piezoelectric material to generate unipolar pressure pulses [6]. When a high step voltage is applied across the piezoelectric material, two unipolar pressure pulses with

Corresponding author; lhwang@biomed.wustl.edu. Phone: (314) 935-6152.
[b]Current address: Department of Electrical Engineering and Computer Science, University of Wisconsin-Milwaukee, Milwaukee, Wisconsin 53201

opposite polarities are generated from the two opposing surfaces of the material. These two unipolar pulses were separated by a time related to the sound velocity in the material and the length of the material being used.

Another method to generate unipolar pressure pulses uses a multi-layered transducer with consecutive time-delayed excitations between layers [8] to produce similar unipolar pulses. However, existing methods are limited in their ability to obtain high ultrasonic pressure due to either the high electrical impedance of thick piezoelement and the high acoustic impedance of the piezocrystals, or to the low piezoelectric coefficient of piezopolymer materials.

The photoacoustic (PA) effect has been later used to generate unipolar pressure pulses [9]. In a homogeneous optically absorbing aqueous solution with a glass boundary, a PA wave was generated due to thermal expansion after a short-pulsed laser irradiation. Near the glass boundary inside the solution, the amplitude of the PA wave decayed exponentially, which followed the optical fluence decay. This decayed wave then propagated in opposite directions (both toward and away from the glass). The wave traveling toward the glass was reflected at the glass-solution interface without a phase change because the acoustic impedance of the glass was much higher than that of the water (rigid boundary condition). As a result, the reflected and the original outward-propagating waves formed a unipolar pressure pulse inside the aqueous solution, which propagated away from the glass. The temporal pulse duration is defined by the solution's optical absorption coefficient and acoustic velocity in the solution; the amplitude is determined by the solution's optical absorption coefficient and the incident optical energy density.

Only plane waves were generated photoacoustically in the aforementioned work; however, focused unipolar pressure waves are required in some specific chemical and biological effects since they require a high concentration of ultrasonic energy within a small volume [4,5]. Focused unipolar pressure pulses are also desired in order to achieve high lateral resolution if they are used for imaging purposes. As described in [10], a short PA pulse was generated by rapid thermoexpansion of a graphite layer deposited on a glass substrate and was subsequently transmitted into the medium. The glass substrate had a concave shape to achieve spherical focusing. However, in the focal region of the transducer this method only produced unipolar displacement rather than unipolar pressure.

In this work, we show mathematically that the temporal profile of a PA pressure wave in the focal region of a spherically focused transducer follows the temporal profile of the laser pulses superimposed with a long pulse of the opposite polarity. We also demonstrate experimentally that quasi-unipolar pressure pulses with a full width at half maximum (FWHM) pulse duration of a fraction of a microsecond were generated around the ultrasonic focus under free boundary conditions (the acoustic impedance of the reflection material is much lower than that of the water).

Theory

Figure 1 shows a short laser pulse with a circular beam profile and an optical fluence F_0 uniformly illuminating an optically absorbing medium through an optically transparent concave window (radius of curvature: R; aperture angle: θ_0). In a homogeneous medium with an optical absorption coefficient μ_a, the optical fluence decays along the direction of the propagation axis z is expressed as $F = F_0 \exp(-\mu_a z)$. Assuming strong optical absorption ($\mu_a R \gg 1$), we can separate the sound generation near the optical window (transducer surface) from the sound generation at the geometrical focal region. The requirement of $\mu_a R \gg 1$ leads to $kR \gg 1$, where k is the acoustic wave number, because peak PA emission occurs at $k \approx \mu_a$ [11]. Under these assumptions small numerical aperture transducers ($\sin \theta_0$

$\ll 1$) can be treated as locally flat. In this case, the PA wave generation can be approximated to a one-dimensional problem.

The one-dimensional transient pressure distribution $p(\mathbf{r}_0)$ induced by the impulse laser excitation is given by

$$p(r_0)=\frac{\beta c^2}{C_p}\mu_a F_0 \exp(\mu_a r_0)=\mu_a \Gamma F_0 \exp(\mu_a r_0),$$

(1)

where β is the isobaric coefficient of volume expansion, c is the sound velocity, C_p is the heat capacity, and $\Gamma = \beta c^2/C_p$ is the Gruneisen parameter [9]. Since the initial particle velocity $v(t = 0, r_0)$ is zero, d'Alembert's solution of Eq. 1 is the sum of two plane waves traveling in opposite directions ($+r_0$ and $-r_0$).

The diverging pressure wave traveling, $p^{(+)}(t, r_0)$, is reflected at the boundary of the transducer. When reflected by a free boundary, the pressure of the wave changes its sign; and when reflected by a rigid boundary, the pressure of the wave keeps its sign.

If the irradiating pulse intensity has a finite temporal duration, $I = I(t)$, the temporal profile of the induced PA pressure pulse can be acquired by convolving the pulse response given by Eq. 1 with the temporal profile of the laser pulse [12]. For diverging PA pressure waves generated from both rigid (denoted as $p_\infty^{(-)}(t, r_0)$) and free (denoted as $p_0^{(-)}(t, r_0)$) boundaries at the transducer surfaces, their temporal profiles become

$$p_\infty^{(-)}(t,R)=\mu_a \Gamma \int_{-\infty}^{\infty} \exp(\mu_a c\,|t-\tau|)I(\tau)d\tau$$

$$p_0^{(-)}(t,R)=\mu_a \Gamma \int_{-\infty}^{\infty} \exp(\mu_a c\,|t-\tau|)(1-2h(t-\tau))I(\tau)d\tau$$

(2)

where $h(t)$ is the Heaviside step function.

It has been shown that the acoustic pressure field $p(t, r_0)$ of a piston source in a rigid planar baffle is related to the normal derivative of the pressure on the radiating surface S at time t_0 [13]. Thus we have

$$p(t,r_0)=\frac{1}{2\pi R}\int_{-\infty}^{+\infty}\int_S \frac{\partial p(t,R)}{\partial n}\Big|_{t_0}\delta(t-t_0-\frac{r}{c})dS\,dt=\frac{1}{2\pi c R}\int_{-\infty}^{+\infty}\int_S \frac{\partial p^{(+)}(t,0)}{\partial t}\Big|_{t_0}\delta(t-t_0-\frac{r}{c})dS\,dt,$$

(3)

where δ is the delta function, and r is the distance from the measuring point, $\mathbf{r}_0$, to the element of the transducer surface dS. By combining Eqs. 2 and 3, we have

$$p_\infty(t, r_0) = \frac{-\mu_a \Gamma}{2\pi cR} \int\limits_{-\infty}^{+\infty} \int\limits_S \frac{\partial p}{\partial t} \int\limits_{-\infty}^{\infty} \exp(-\mu_a c |t - \tau|) I(\tau) d\tau \Big|_{t_0} \delta(t - t_0 - r/c) dS \, dt = \frac{\mu_a \Gamma}{2\pi cR} \int\limits_{-\infty}^{+\infty} \int\limits_S \int\limits_{-\infty}^{\infty} \mu_a c \exp(-\mu_a c |t - \tau|)(1 - 2h(t - \tau)) I(\tau) d\tau \Big|_{t_0} \delta(t - t_0 -$$

$$p_0(t, r_0) = \frac{-\mu_a \Gamma}{2\pi cR} \int\limits_{-\infty}^{+\infty} \int\limits_S \frac{\partial p}{\partial t} \int\limits_{-\infty}^{\infty} \exp(-\mu_a c |t - \tau|)(1 - 2h(t - \tau)) I(\tau) d\tau \Big|_{t_0} \delta(t - t_0 - r/c) dS \, dt = \frac{\mu_a \Gamma}{2\pi cR} \int\limits_{-\infty}^{+\infty} \int\limits_S (\int\limits_{-\infty}^{\infty} \mu_a c \exp(-\mu_a c |t - \tau|) I(\tau) d\tau - 2I(t)) \Big|_{t_C}$$

(4)

For a free boundary, the solution is the sum of two pressure waves. The first wave is predominantly defined by the spatial distribution of the optical energy deposition $\exp(\mu_a r)$ and the sound velocity. The second wave is defined by the temporal profile of the laser pulse. In the ultrasonic focal region, Eq. 4 can be further evaluated as

$$p_\infty(t, 0) = \mu_a^2 \Gamma R(1 - \cos\theta_0) \int\limits_{-\infty}^{\infty} \exp(-\mu_a c |t - R/c - \tau|)(1 - 2h(t - R/c - \tau)) I(\tau) d\tau$$

$$p_0(t, 0) = \mu_a^2 \Gamma R(1 - \cos\theta_0) \left[\int\limits_{-\infty}^{\infty} \exp(-\mu_a c |t - R/c - \tau|) I(\tau) d\tau - 2(\mu_a/c) I(t - R/c) \right].$$

(5)

The temporal profile of a laser pulse is frequently approximated by a Gaussian function [9]:

$$I(t) = \frac{1}{\sqrt{\pi}} \frac{F_0}{\tau_H} \exp(-(\frac{t}{\tau_H})^2), \text{ where } \tau_H \mu_a c \ll 1.$$

(6)

In this case, the approximation for a pressure pulse at the focus of the transducer can be written explicitly as

$$p_\infty(t, 0) \approx (\mu_a R(1 - \cos\theta_0)) \cdot \mu_a F_0 \Gamma \{ \exp(-\mu_a c |t - R/c|)(1 - 2h(t - R/c)) \}$$

$$p_0(t, 0) \approx (\mu_a R(1 - \cos\theta_0)) \mu_a F_0 \Gamma \left\{ \exp(-\mu_a c |t - R/c|) - \frac{2}{\mu_a c \sqrt{\pi}\tau_H} \exp(-(\frac{t}{\tau_H})^2) \right\}.$$

(7)

For a rigid boundary, the acoustic pressure in the focal region is equal to the sound pressure of a PA wave generated by a free boundary planar transducer multiplied by a pressure amplification factor $\mu_a R(1 - \cos\theta_0)$ [14], in which μ_a plays the role of wavenumber k. Moreover, the pressure amplitude changes from positive to negative near $t = R/c$.

For the free boundary transducer, the acoustic pressure in the focal region is equal to the sum of the positive sound pressure, as if it were generated by a planar rigid boundary transducer, and a negative pressure pulse with the temporal profile of the laser pulse. For a Gaussian pulse, the amplitude ratio of the negative to positive pressure peaks, $2/(\mu_a \tau_H c \sqrt{\pi})$, is defined by the ratio of the characteristic times for optical energy deposition, $1/(\mu_a c)$, and the width of the laser pulse $2\sqrt{\ln(2)} \cdot \tau_H$. Again, the amplitude of both components is multiplied by a pressure amplification factor.

Experimental results

The schematic of the experimental setup is shown in Figure 2a. A Nd:YAG laser (Brilliant, Big Sky) generated laser pulses (pulse duration: 20 ns; pulse energy: 50 mJ) at 532 nm with a pulse repetition rate of 10 Hz. The laser pulses were expanded by a negative lens, homogenized by a narrow angle ground glass diffuser (DG10-15000, Thorlabs), and shaped by a 20-mm diameter iris diaphragm. The laser pulses then passed through an optically transparent backing and entered an optically absorbing medium. The backing and the dye together acted as a PA transducer.

To create a rigid boundary, an SF2 glass, plano-concave lens (R=85 mm) was used as the backing medium, and an aqueous solution of Sudan Red dye was used as the optical absorbing medium (Figure 2b). The optical absorption coefficient of the dye solution was 0.5 mm^{-1}. To create a free boundary, air backing was used and the aqueous solution was replaced by a 2% water-based agar gel block made from the same dye concentration (Figure 2c). The gel maintained its shape in the outer boundary of the PA transducer and allowed the use of air backing in experiments. Figure 2b and Figure 2c show only the concave boundary. When a planar boundary was required, the plano-concave lens was replaced by an optical window (rigid boundary), and the convex gel block was replaced by a flat gel block (free boundary).

The particle displacement velocity of the ultrasonic pulse was measured at the water surface of the PA transducers by a laser vibrometer (OFV 5000, Polytech) equipped with an ODV 505 super heterodyne interferometer head, a VD-05 10-MHz velocity detector, and a DD-300 20-MHz displacement decoder. The detection head was mounted on a translational stage to laterally position its 50-μm diameter measurement point along the propagating axis of the induced PA waves (z axis). Axial positioning was achieved by changing the water level in the PA transducer. The velocity of the free water surface was twice that of the normal component of the particle displacement velocity. For $kR \gg 1$, the particle displacement velocity is proportional to the acoustic pressure near the ultrasonic focus [14]; thus, we have

$$v(t,0) \approx \frac{p(t,0)}{\rho c}\left(\frac{(1+\cos\theta_0)}{2} - \frac{\cos^2\theta_0}{ikR}\right) \approx \frac{(1+\cos\theta_0)}{2}\frac{p(t,0)}{\rho c}.$$

(8)

Correspondingly, the output of the vibrometer velocity decoder (or derivative of the output voltage of the displacement decoder) is proportional to the acoustic pressure at the measuring location.

Figure 3 shows the temporal pressure profiles of the PA pulses from the flat and focused PA transducers with rigid boundaries. In Figure 3a, the temporal profile of the near field of the flat PA transducer has two conjunct exponential exponents, which is similar to the temporal profile reported in [9]. Additional spikes appearing with ~0.1 μs delay from the pressure peak are likely caused by edge effects due to the finite size of the transducer [10].

Figure 3b shows the temporal profiles of the PA waves at different locations along the propagation axis for the focused PA transducer (as shown in Figure 2b). Different traces correspond to different axial positions of the measurement points. At positions close to the concave interface, the temporal profiles of the PA pressure waves are identical to the profile in the flat transducer shown in Figure 3a. However, Eq. 7 indicates that the temporal profile of the acoustic pressure in the geometrical focus can be approximated by the first derivative of the signal profile close to the interface. Accordingly, we observed that the temporal

profile of the PA pressure wave at the geometrical focus became bipolar, which is the derivative of the temporal profile of the wave shown in Figure 3a. Moreover, Figure 3b also shows that the signal magnitude becomes much higher due to energy concentrated in the focal area. Signal oscillations after a steep change of signal voltage are caused by the finite bandwidth of the vibrometer.

Figure 4 shows the temporal profiles of the PA wave generated from the transducer with a free boundary. The pressure pulse shown in Figure 4a was measured from the flat transducer, which has a shape similar to that reported elsewhere [9]. However, the pressure pulse on the axis of the spherically focused transducer near the focal region becomes quasi-unipolar, as shown in Figure 4b. Such a quasi-unipolar temporal profile can be considered as the first derivative of the temporal profile shown in Figure 4a, based on Eq. 7. The ratio of the negative to positive peak magnitudes of the pressure pulse is in good agreement with the theoretical calculation. Additional oscillations of the pressure pulse after reaching its main negative peak were caused by a high order low-pass filter of the vibrometer cut-off frequency, which is within the signal bandwidth. Since the time-average of the pressure pulse in the free space must be zero, and the amplitude of the negative part is much larger than that of the positive part, the positive part has a much longer duration than that of the negative part.

Conclusions

We have demonstrated both theoretically and experimentally the PA generation of quasi-unipolar focused pressure pulses. Because the temporal profile of a pressure pulse at the geometrical focus can be approximated by the first derivative of the temporal profile near the boundary, in order to achieve quasi-unipolar pressure at the ultrasonic focus, bipolar pressure is required at the boundary.

In the experiments, we built spherically focused PA transducers with both free and rigid boundaries. The detected temporal profiles at the boundaries and at the geometrical focuses agreed with theoretical estimations. In the focused PA transducer with a free boundary, a quasi-unipolar pressure pulse was generated in the focal region. Such a quasi-unipolar pulse is a superposition of two parts: a positive part with an exponential rise and decay with a time constant of $1/\mu_a c$, and a negative part following the temporal profile of the laser pulse. The ratio of the magnitudes of negative to positive counterparts of the pressure pulse for a Gaussian pulse can be approximated by $2/(\mu_a c \tau_H \sqrt{\pi})$. By properly choosing the absorption coefficient of the solution in the PA transducer and the pulse duration of the laser excitation, it is possible to control the ratio of the positive and negative parts of the quasi-unipolar pressure pulse.

Acknowledgments

References

1. Hariti SA, Hole S, Lewiner J. Broadening the potential bandwidth of piezoelectric transducers by partial depolarization. Appl. Phys. Lett 2001;78:4037–4039.

2. DeBilly M, Adler L, Quentin G. About the use of trailing echoes for the detection of disbond at solid-solid interface. J. Phys 1994;4:917–921.

3. Sotiropoulos DA, Achenbach JD. Reflection of elastic-waves by a distribution of coplanar cracks. J. Acoust. Soc. Am 1988;84:752–759.

4. Church CC. A theoretical study of acoustic cavitation produced by "positive-only" and "negative-only" pressure waves in relation to *in vivo* studies. Ultrasound in Med. & Biol 2003;29:319–330. [PubMed: 12659920]

5. Dalecki D, et al. Bioeffects of positive and negative acoustic pressures in mice infused with microbubbles. Ultrasound in Med. & Biol 2000;26:1327–1332. [PubMed: 11120371]

6. Peterson RG, Rosen M. Use of the thick transducers to generate short duration stress pulses in thin specimens. J. Acoust. Soc. Am 1967;41:336–345.

7. Foster FS, Hunt JW. The design and characterization of short pulse ultrasound transducers. Ultrasonics 1978;16:116–122.

8. Sferruzza JP, Birer A, Cathignol D. Generation of very high pressure pulses at the surface of a sandwiched piezoelectric material. Ultrasonics 2000;38:965–968. [PubMed: 11106008]

9. Oraevsky AA, Jacques SL, Tittel FK. Measurement of tissue optical properties by time-resolved detection of laser-induced transient stress. Appl. Opt 1997;36:402–415. [PubMed: 18250688]

10. Fomitchov PA, Kromine AK, Krishnaswamy S. Photoacoustic probes for nondestructive testing and biomedical applications. Appl. Opt 2002;41:4451–4459. [PubMed: 12153070]

11. Calasso IG, Craig W, Diebold GJ. Photoacoustic point source. Phys. Rev. Let 2001;86:3550–3553. [PubMed: 11328020]

12. Stepanishen PR. Transient radiation from pistons in an infinite planar baffle. J. Acoust. Soc. Am 1971;49:1629–1638.

13. Morse, PM.; Ingard, KV. Theoretical Acoustics. New York: McGraw-Hill; 1968. p. 322

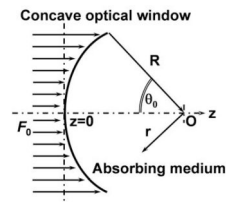14. O'Neil H. Theory of focusing radiators. J. Acoust. Soc. Amer 1949;21:516–526.

Figure 1.
Geometry of the theoretical model. F_0: optical fluence; θ_0 : aperture angle; R : radius of curvature; O: center of the spherical surface.
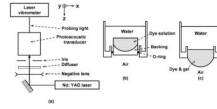
Figure 2.
The schematic of the experimental setup for quasi-unipolar pressure pulse generation is given in (a); the designs of PA transducers with rigid and free boundaries are shown in (b) and (c), respectively.
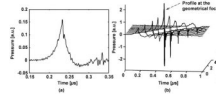
Figure 3.
Temporal profiles of pressure pulses from the PA transducers with rigid boundaries. (a) The temporal profile of the near field of a flat transducer; (b) The temporal profiles along the wave propagation axis while the pressure pulse propagates through the focal region of the spherically focused transducer. The shorter distance indicates the measuring position is closer to the boundary. The distance 0 indicates the first measuring position, which is around 83 mm away from the boundary.
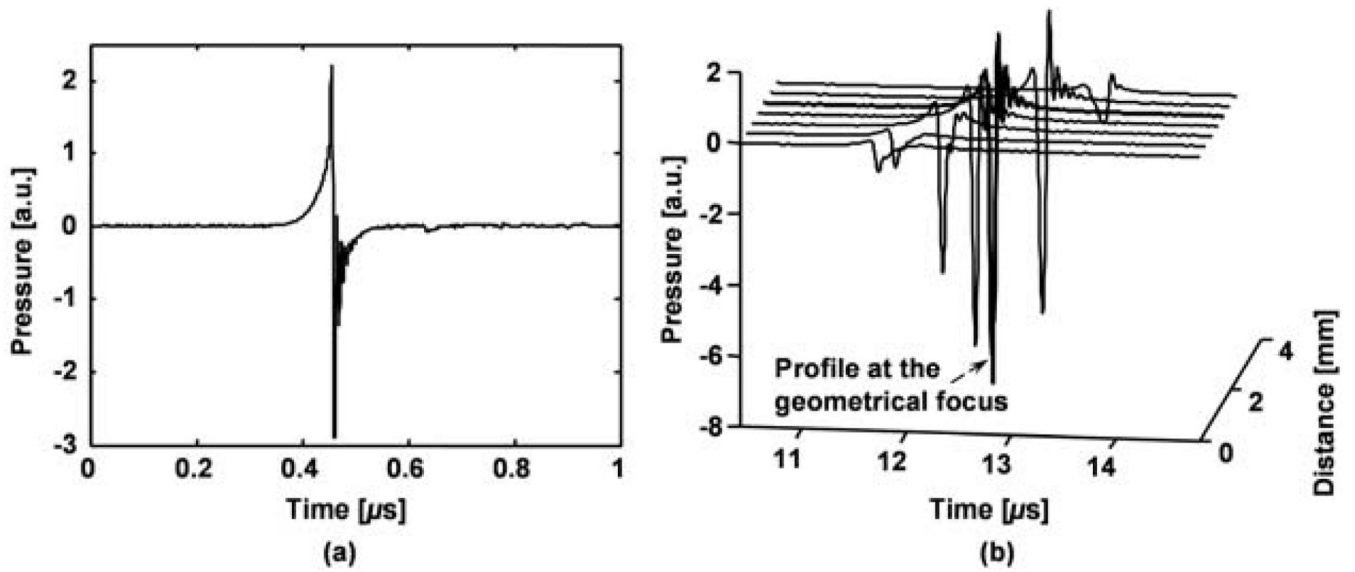
Figure 4.
Temporal profiles of pressure pulses from the PA transducers with free boundaries. (a) Narrow field, plane geometry; (b) Change of the temporal profiles while the pressure pulse propagates through the focal region of the spherical transducer.